

# Preparation and characterization of poly(urea-formaldehyde) microcapsules filled with epoxy resins

Li Yuan, Guozheng Liang\*, JianQiang Xie, Lan Li, Jing Guo

*Department of Applied Chemistry, School of Science, Northwestern Polytechnical University, xi'an 710072, People's Republic of China*

Received 23 March 2006; received in revised form 11 May 2006; accepted 25 May 2006

Available online 13 June 2006

## Abstract

The preparation of microcapsules applied to the fabrication of self-healing composites has been paid more attentions. A new series of microcapsules were prepared by in situ polymerization technology with poly(urea-formaldehyde) (PUF) as a shell material and a mixture of epoxy resins (diglycidyl ether of bisphenol A: DGEBA) and 1-butyl glycidyl ether (BGE) as core materials. The microencapsulating process of core material was monitored using optical microscopy (OM). The chemical structure of microcapsule was characterized using Fourier-transform infrared spectroscopy (FTIR). Morphology and shell wall thickness of microcapsule were observed using metalloscope (MS), scanning electron microscopy (SEM) and OM, respectively. The effects of different pre-polymers, weight ratios of urea to formaldehyde (U–F) and the agitation rates on the physical properties of microcapsules were investigated. The storage stability of microcapsules at different times and temperatures was analyzed. The thermal properties of microcapsules were investigated using differential scanning calorimetry (DSC) and thermogravimetric analysis (TGA). The results indicate that PUF microcapsules containing epoxy resins can be synthesized successfully, and during the microencapsulation, the epoxide rings in epoxy resins are hardly affected by the surrounding media. The rough outer surface of microcapsule is composed of agglomerated PUF nanoparticles. The size and surface morphology of microcapsule can be controlled by selecting different processing parameters. The microcapsules basically exhibit good storage stability at room temperature, and they are chemically stable before the heating temperature is up to approximately 238 °C.

© 2006 Elsevier Ltd. All rights reserved.

*Keywords:* Microcapsule; Epoxy resins; Poly(urea-formaldehyde) (PUF)

## 1. Introduction

The existing microcapsules have been applied to many fields such as in pharmaceuticals [1,2], food additives [3], coatings [4,5], electronic inks [6,7], catalysts [8], dyes [9,10], etc. because the core materials such as drugs, water, dyes or oils can be protected by the shell of microcapsules from the damages of environment or can be released under a controlled condition. In order to develop new, versatile applications of microcapsules, the synthesis and characterization of microcapsules have been researched extensively. Recently, a new application of poly(urea-formaldehyde) (PUF) microcapsules containing dicyclopentadiene (DCPD), which are synthesized by in situ polymerization technology, has been developed to fabricate self-healing polymeric composites based on epoxy matrix [11–13]. The PUF microencapsulated polystyrene and

styrene as healing agents have also been developed for self-healing polyester matrix composite [14]. The self-healing mechanism of polymeric composites is inspired by biological system. Microcapsules filled with healing agents are dispersed throughout a polymer matrix, they are ruptured by the propagation of microcrack when damage occurs in the matrix, and the healing agent is released into the crack by capillary action. The polymerization of healing agent is triggered by contact with an embedded catalyst or curing agent and bonds the crack faces closed [12]. As a result, the damaged polymeric composites are repaired. The microcapsules filled with healing agents embedded in composites are special, they must remain intact during the fabrication processing of composites, rupture when propagating microcracks occur and release the healing agent. All these microcapsules filled with healing agents offer tremendous potential for providing long-lived structural materials and saving time and manpower used in repairing composites. Therefore, microencapsulated liquid healing agents, which can be used to fabricate self-healing composites, have been paid more attentions.

\* Corresponding author. Tel.: +86 29 88474080; fax: +86 29 88474080.  
E-mail address: [lgzheng@nwpu.edu.cn](mailto:lgzheng@nwpu.edu.cn) (G. Liang).

Epoxy resins are reactive monomers and can be reacted with wide variety of curing agents or hardeners such as amines of differential functionalities and anhydrides at different temperatures. They are extensively used in many applications such as surface coating, adhesive, and laminates for composite materials due to excellent mechanical resistance of the cured products and good adhesion to many substrates [15–20]. So, they may be used as healing agents for the fabrication of self-healing composites. Moreover, high thermal decomposition temperature of epoxy resins may endow microcapsules with higher thermal stability. The commercial epoxy resins always have high viscosity, and cannot be used as healing agents directly for the failing capillarity action in the microcracks, but adding reactive diluents can decrease the viscosity of epoxy resins. When the addition of the reactive diluents is about 20 wt% of epoxy resins, the viscosity of epoxy resins is decreased dramatically and the mechanical properties of cured products can basically remain [15,17,21], compared with the virgin epoxy resins. Therefore, epoxy resins containing 0–20 wt% reactive diluents can be the candidate of self-healing agent.

In this study, we adopted in situ polymerization technology in an oil-in-water emulsion to prepare PUF microcapsules filled with a mixture of diglycidyl ether of bisphenol A (DGEBA) and 1-butyl glycidyl ether (BGE). Detailed descriptions of the fabrication process and the fabrication conditions for PUF microcapsules had been reported in many literatures [22–24]. The PUF microcapsules filled with a mixture of DGEBA and BGE were characterized by Fourier-transform infrared (FTIR) spectroscopy, scanning electronic microscope (SEM), optical microscope (OM), metaloscope (MS), differential scanning calorimeter (DSC) and thermogravimetric analyser (TGA) to investigate their chemical structure, surface morphology, size distribution and thermal stability, respectively.

## 2. Experimental

### 2.1. Materials

Epoxy resins (diglycidyl ether of bisphenol A: DGEBA (E-51, epoxide equivalent weight: 196 g/mol)) used as core material was purchased from Wuxi Resin Plant, China. 1-Butyl glycidyl ether (BGE) used as reactive diluent of DGEBA, was purchased from Shanghai Resin Plant, China. Urea (U) and 37 wt% formaldehyde (F) used as shell materials were purchased from Tianjin Chemical Plant, China. Triethanolamine (TEA), used to control the pH of solution, and sodium dodecylbenzene sulfonate (SDBS) (99% purity), used as emulsifier, were purchased from Tianjin Chemical Regents Factory, China. 10 wt% sulfuric acid solution was prepared in our laboratory to control the pH of emulsion. Fig. 1 shows the chemical structure of DGEBA, BGE, U, F and TEA.

### 2.2. Preparation of microcapsules

PUF microcapsules were prepared by the following two-step process:

- (1) At room temperature (20–25 °C), U, F and deionized water were mixed in a 250 ml three-neck round-bottomed flask connected to a reflux condenser and equipped with a mechanical stirrer. After the urea dissolved, the pH of solution was adjusted to 8–9 with TEA and temperature was kept at 60–70 °C for 1 h, then the U–F pre-polymer solution was obtained. Fig. 2(a) shows the reaction scheme of the formation of U–F in alkaline media.
- (2) Under agitation, 100 ml of 2 wt% aqueous solution of SDBS was added to the as prepared pre-polymer solution, and then a slow stream of a prepared mixture of DGEBA and BGE (weight ratio of BGE to DGEBA: 0.2) was added to form an oil in water (O/W) emulsion. After stirred for 20–30 min, the pH of the emulsion was adjusted slowly

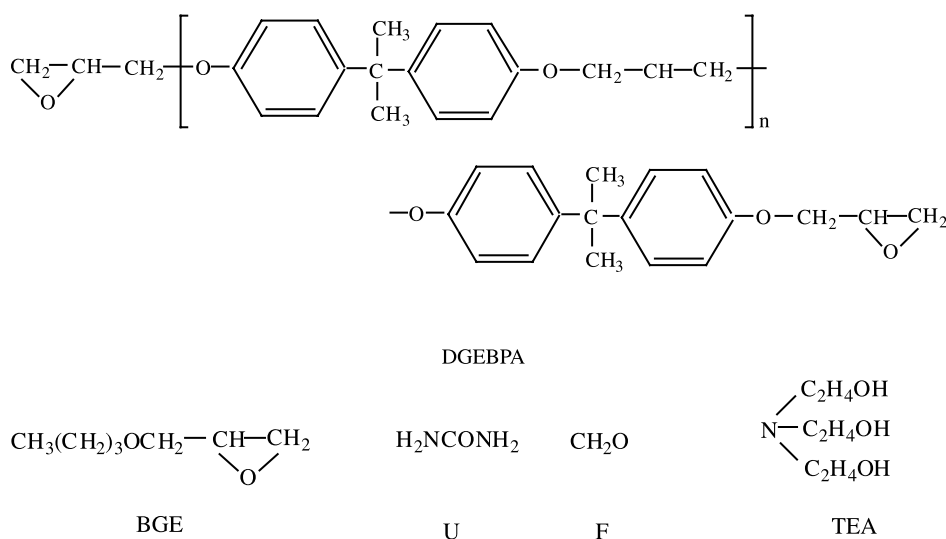


Fig. 1. Chemical structure of the materials used in this work.

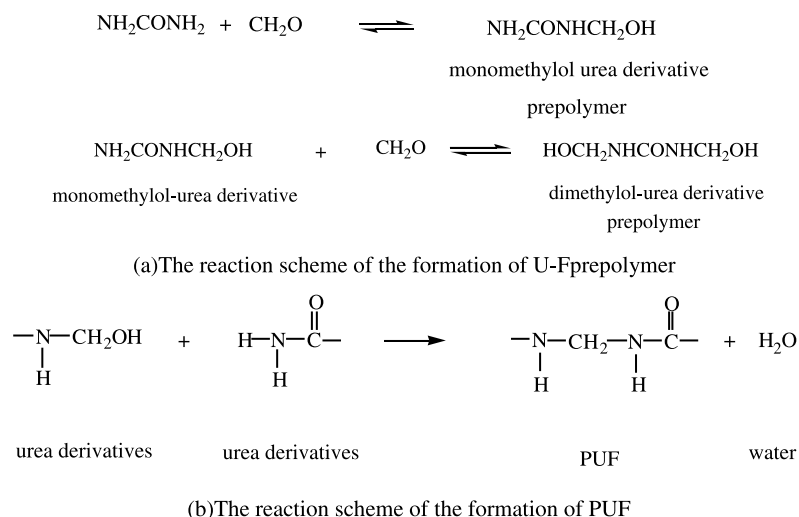


Fig. 2. The reaction scheme of U–F resins. (a) The reaction scheme of the formation of U–F pre-polymer. (b)The reaction scheme of the formation of PUF.

to 3–4 by 10 wt% sulfuric acid solution while the solution was slowly heated to the target temperature of 60–65 °C. After 3 h, the reaction was ended. The obtained suspension of microcapsules was cooled down to ambient temperature, rinsed with deionized water and acetone, filtered and air-dried for 24 h. Fig. 2(b) shows the condensation reaction scheme of U–F resins. Table 1 represents the composition of microcapsules prepared at different processing parameters.

### 2.3. Characterization

Fourier-transform infrared (FTIR) spectra were obtained using a FTIR spectrometer (WQF-310, Beijing Optical Instrument Factory) to identify the chemical structure of the specimen, which was prepared by grinding the sample with a potassium bromide (KBr) or by attaching sample to a KBr disc.

The surface morphology of microcapsule was observed using a scanning electronic microscope (SEM, QUANTA200, FEI). One drop of the microcapsules dispersion was placed on a

stainless steel stub and allowed to air-dry overnight, and then the samples were sputtered with a thin layer (about 10 nm) of gold. The morphology of microcapsules also was observed using optical microscope (OM, XSP-XSZ, Beijing Tech Instrument Co., Ltd, China) and metalloscope (MS, PM-T3, OLYMPUS).

The microcapsule size distribution was investigated using OM technology, and size analysis was performed using OM on data sets of at least 250 measurements. The microcapsule shell thickness was measured by the following steps using OM: the microcapsule specimens were embedded in an epoxy matrix, which are cured at room temperature, ruptured with a razor blade to facilitated membrane sample, and then the sample was mounted on a glass plate to observe.

The storage stability is crucial to the applications of microcapsules. Their storage stability was characterized by the weight loss of microcapsules exposed to room temperature at periodic intervals and heat-treated for 4 or 8 h at different temperatures, respectively.

The thermal stability of microcapsule was measured using thermogravimetric analysis (TGA, Q50, TA) at a heating rate

Table 1  
The composition of microcapsule prepared at different processing parameters

Sample no.	Weight ratio of U–F	Weight ratio of core–shell material	Agitation rate (rpm)	Measured core content ( $W_{V_{\text{core}_1}}$ )	Yield (%)
1–1	0.750	1.00	325	72.3	< 19.0
1–2	0.500	1.00	325	77.6	96.0
1–3	0.375	1.00	325	76.5	94.9
2–1	0.500	0.50	380	51.7	80.0
2–2	0.500	0.75	380	66.5	85.0
2–3	0.500	1.00	380	76.5	95.0
2–4	0.500	1.25	380	77.4	97.0
2–5	0.500	1.50	380	90.4	86.0
2–6	0.500	2.00	380	91.0	70.0
3–1	0.500	1.00	200	91.9	77.0
3–2	0.500	1.00	250	96.3	79.0
3–3	0.500	1.00	300	78.2	84.0
3–4	0.500	1.00	350	77.7	96.0
3–5	0.500	1.00	400	76.9	93.0
3–6	0.500	1.00	500	76.5	88.0

of 10 °C/min and differential scanning calorimetry (DSC, 2910 MDSC, TA) at a heating rate of 10 °C/min in a nitrogen atmosphere.

#### 2.4. Determination of content of epoxide ring

Quantitative estimation of characteristic group can be obtained by FTIR using internal standards. During the microencapsulation process, the phenyl ring cannot be affected by the media and its band can be selected as reference band. The relative content of epoxide ring of microcapsules can be evaluated by the following equation

$$W_{M \text{ epoxide ring}} = \frac{S_{M \text{ epoxide ring}}/S_{M \text{ Ph}}}{S_{0 \text{ epoxide ring}}/S_{0 \text{ Ph}}} \times 100\% \quad (1)$$

where  $W_{M \text{ epoxide ring}}$  is the relative content of epoxide ring of microcapsule samples.  $W_{M \text{ epoxide ring}}$  and  $S_{M \text{ Ph}}$  are the integral areas of characteristic peaks of epoxide ring at about 910  $\text{cm}^{-1}$  and phenyl ring at about 1610  $\text{cm}^{-1}$  of microcapsule samples, respectively.  $W_{0 \text{ epoxide ring}}$  and  $S_{0 \text{ Ph}}$  are the integral area of characteristic peaks of epoxide ring at about 910  $\text{cm}^{-1}$  and phenyl ring at about 1610  $\text{cm}^{-1}$  of the mixture of DGEBA and BGE.

#### 2.5. Determination of core content of microcapsule

The prepared microcapsule core content was determined by extracting method and using acetone as extracting solvent. Microcapsule samples were grinded with a pestle in a mortar at room temperature. The crushed microcapsules were collected and washed with acetone several times, then dried at room temperature. Knowing the initial weight of intact

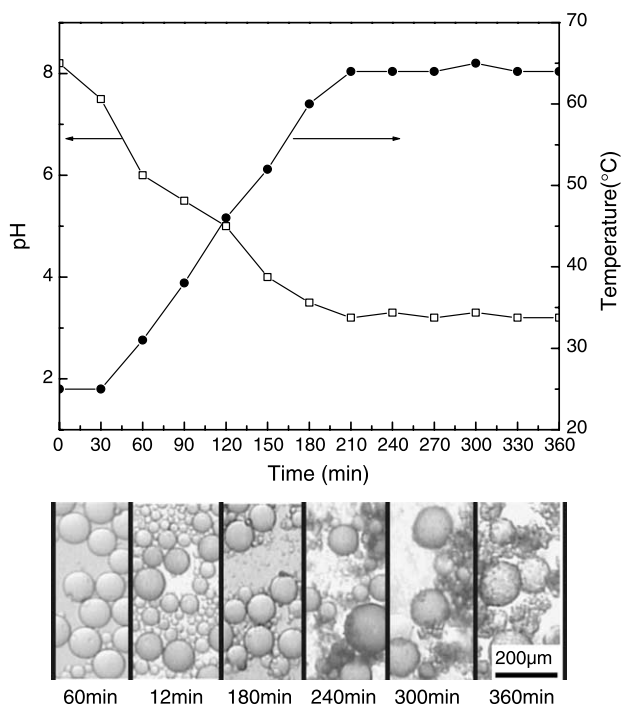


Fig. 3. The microencapsulation process along with temperature and pH.

microcapsules ( $W_{M_i}$ ) and the weight of residual wall shell ( $W_{UF_i}$ ) of microcapsules, the wall shell content ( $W_{V_{UF_i}}$ ) and core content ( $W_{V_{core_i}}$ ) of microcapsule were calculated as

$$W_{V_{UF_i}} = \frac{W_{UF_i}}{W_0 M} \times 100\% \quad (2)$$

$$W_{V_{core_i}} = 1 - W_{V_{UF_i}} \quad (3)$$

### 3. Results and discussion

#### 3.1. Microencapsulation process

The microencapsulation process of core material of microcapsule sample no. 1–2 was monitored by OM. Fig. 3 shows a sequence of aliquot images along with the temperature

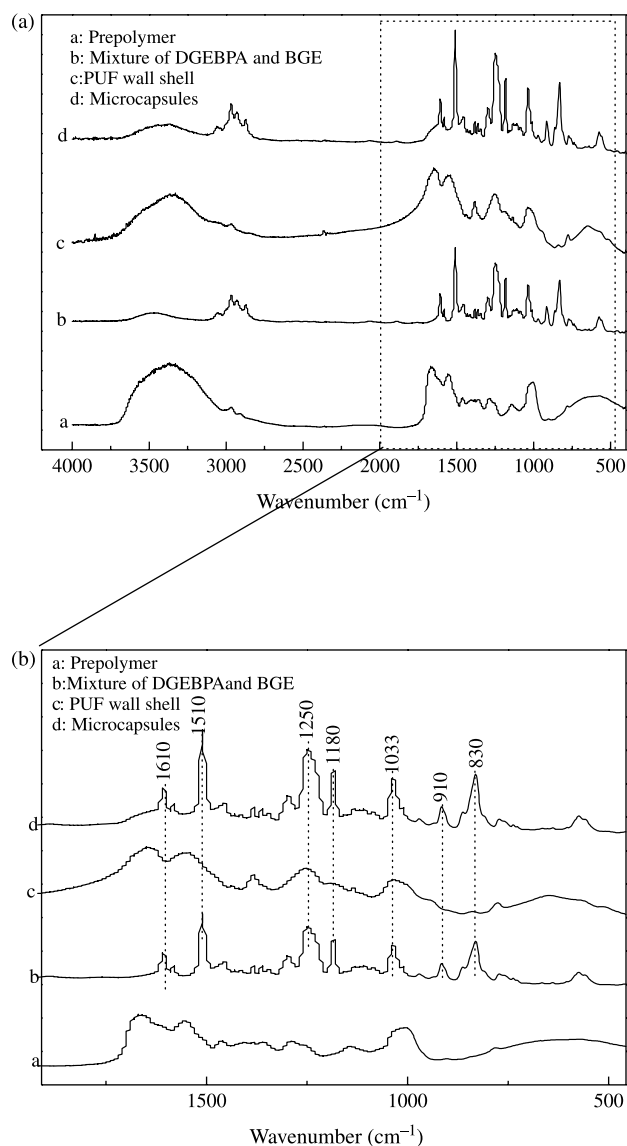


Fig. 4. FTIR spectra: (a) prepolymer; (b) DGEBA and BGE; (c) PUF wall shell; (d) PUF microcapsules containing DGEBA and BGE.

Table 2  
Wavenumbers ( $\text{cm}^{-1}$ ) and assignments of the FTIR spectra of the mixture of DGEBPA and BGE, PUF pre-polymer and PUF wall shell

DGEBPA	Approximate assignment	BGE	Approximate assignment	Pre-polymer/ PUF wall shell material	Approximate assignment
3610–3339	$\nu\text{O-H}$	2873–2964	$\nu\text{C-H}$ (methyl group)	3707–3050	$\nu\text{N-H}$ $\nu\text{O-H}$
3000–3100	$=\text{CH}$ (phenyl ring)	1033	$-\text{C-O-C}-$	1649	$\begin{array}{c} \text{O} \\ \parallel \\ -\text{NH}-\text{C}-\text{NH}- \end{array}$
1610	$\nu\text{C}=\text{C}$ (phenyl ring)	1180	$\text{C}-\text{C}-\text{C}$ 	1544	$\begin{array}{c} \text{O} \\ \parallel \\ -\text{C}-\text{NH}- \end{array}$
1510	$-\text{C-O-C}-$ (phenyl ring)	910	$-\text{CH}-\text{CH}_2$   O	1027	$-\text{C}-\text{O}-\text{C}$   
1250	$-\text{C-O-C}-$	830			
910	$-\text{CH}-\text{CH}_2$   O				
830					

and pH value. After the addition of epoxy resins, the solution temperature is increased slowly and the pH of solution is adjusted from 8.5 to 6, the epoxy resins droplets can be observed in the time range of 0–60 min. During the period of 60–120 min, as the pH value decreases and the temperature increases, the solution becomes a cloudy emulsion and then transforms a milk white emulsion owing to the increase of the molecular weight of pre-polymer and the development of PUF nanoparticles in suspension. The microcapsules appear during 120–180 min, at temperatures between 45–60 °C and at pH value of 3.5–5 due to the deposition of PUF nanoparticles yielded by a part of pre-polymer. Distinct microcapsules can be observed during 180–240 min, at temperatures between 60–65 °C and at pH of 3.2–3.5, but the microcapsules are easily fractured or deformed if the agitation is stopped, the reason is the thinner wall shell of microcapsules and uncompleted microencapsulation of core material. Stabilizing the temperature and pH during the period of 240–300 min, the shell of microcapsule becomes thick owing to the further reaction of pre-polymer and the deposition of PUF nanoparticles at the core–water interface. The wall shell thickness reaches its maximum during 300–360 min, the suspension becomes clear and microcapsules can be easily separated.

### 3.2. Chemical structure of microcapsule

Fig. 4 shows the FTIR spectra of pre-polymer, a mixture of DGEBPA and BGE, PUF wall shell material and microcapsule sample no. 1–2. Table 2 lists the detailed peak assignments of the mixture of DGEBPA and BGE, PUF pre-polymer and PUF wall shell material. Obviously, the FTIR spectrum of PUF microcapsules containing the mixture of DGEBPA and BGE (curve (d) in Fig. 4) displays a absorption peak of  $\begin{array}{c} -\text{CH}-\text{CH}_2 \\ | \\ \text{O} \end{array}$  at 910 and 830  $\text{cm}^{-1}$ , indicating that the PUF microcapsules are filled with the mixture of DGEBPA and BGE.

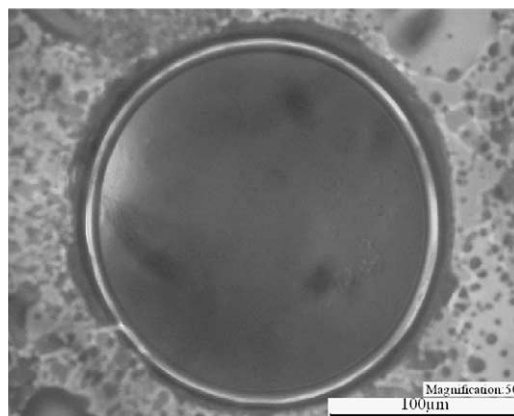


Fig. 5. OM micrograph of prepared microcapsule.

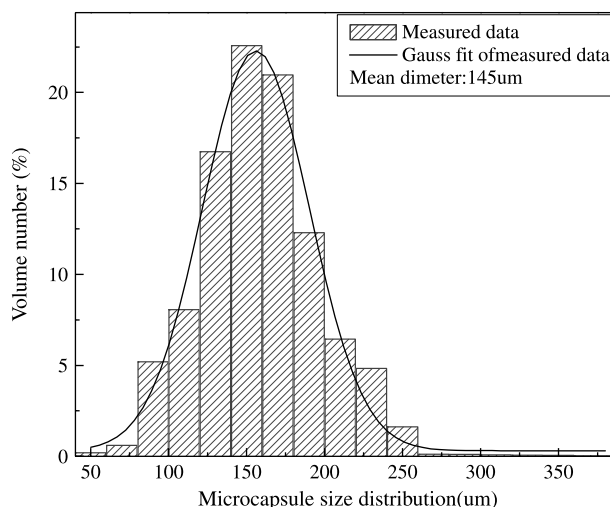


Fig. 6. Size distribution of microcapsule sample no. 1–2.





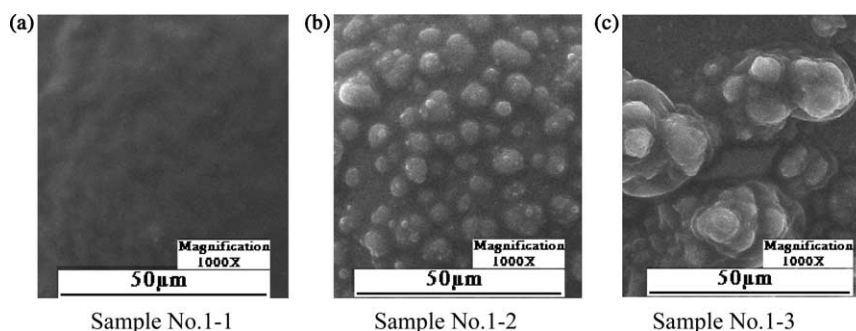


Fig. 11. Surface morphologies of microcapsules (samples no. 1–1 to 1–3).

the propeller blades, many smaller microeddies exist, which result in a wider length scale [25,26]. The microcapsule size can be controlled by the adjusting agitation rate. In this study, the mean diameter of the prepared microcapsules is 145  $\mu\text{m}$ .

### 3.4. Microcapsule surface morphology

Fig. 7 shows the SEM micrograph of microcapsule sample no. 1–2. The surface of microcapsule is rough and scraggly, and it is composed of PUF nanoparticles protruding from the surface. The protuberant nanoparticles can increase the surface areas of microcapsules and enhance surface adhesion [11]. In Fig. 7, microcapsule, PUF nanoparticle agglomerates and the broken wall shell are labeled, respectively.

### 3.5. Microcapsule shell thickness

Wall shell thickness of microcapsule, which determines the mechanical properties of microcapsule and the release model of core material, largely depends on the manufacturing parameters such as the ratio of core–shell material, agitation rate and so on. Fig. 8 shows the OM micrographs of microcapsule sample no. 1–2 embedded in epoxy matrix. The black ring area represents the wall shell material. In this study, the wall thickness of microcapsule sample no. 1–2 falls consistently between 5 and 82  $\mu\text{m}$ .

### 3.6. Effects of different polar pre-polymer

During the microencapsulation process of epoxy resins, epoxy rings may be affected by the surrounding medium and the decrease of epoxide ring may fail the applications of microcapsules. So, the content of epoxide ring must be considered. Epoxy resins are probably affected by the basic solution in the initial stage of the microencapsulation process and Fig. 9(a) shows the reaction mechanism of epoxy resin in basic solution. The self-etherification reaction of epoxy resins may occur between the hydroxyl group and epoxide group at acid pH and Fig. 9(b) shows the self-etherification mechanism of epoxy resins in acid solution. The mono and dimethylol urea-derivatives are the most common products among the U–F pre-polymers. Although the urea group can accelerate the curing reaction of epoxy resins [27–29], the previous studies find no evidence of thermal dissociation in the reactions of

dimethylamine-derived urea with DGEBA [30]. According to the results reported by the Refs. [20,31,32], epoxy resins hardly react with urea-derivatives at lower temperature because the reactivity between epoxide ring and  $-\text{NH}-$  group in urea-derivative is very low below 200  $^{\circ}\text{C}$  unless catalyst is used. So, the influences of urea-derivatives on epoxide ring can be neglected. The relative epoxide ring contents of microcapsule samples no. 1–1, 1–2 and 1–3 obtained by Eq. (1) and FTIR of microcapsules and the mixture of DGEBA and BGE (Figs. 4 and 10) are 99.5, 99.6 and 99.9%, respectively, which indicates that epoxy ring is affected slightly during the microencapsulation process in despite of different pre-polymers. The main reason may be the fact that in an heterogeneous system, where reaction takes place at the interphase, stoichiometry is no longer maintained, critical conversion becomes topology dependent [33,34]. Additionally, the alkali and acid are extremely small amount in solution.

Fig. 11 shows the SEM micrographs of microcapsule surfaces. As the U–F weight ratio decreases, the surface of microcapsule gradually gets rough. In general, when the weight ratio of U–F is lower, the content of free-formaldehyde is higher, although the network density of PUF decreases, the condensation rate of U and F increases [35,36], which results in the quick deposition of PUF nanoparticle on the surface of

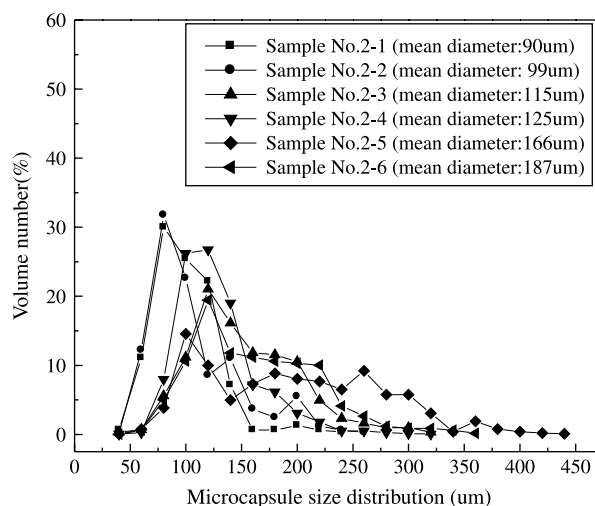


Fig. 12. Size distributions of microcapsules with different weight ratios of core–shell materials along with the mean diameters (samples no. 2–1 to 2–6).

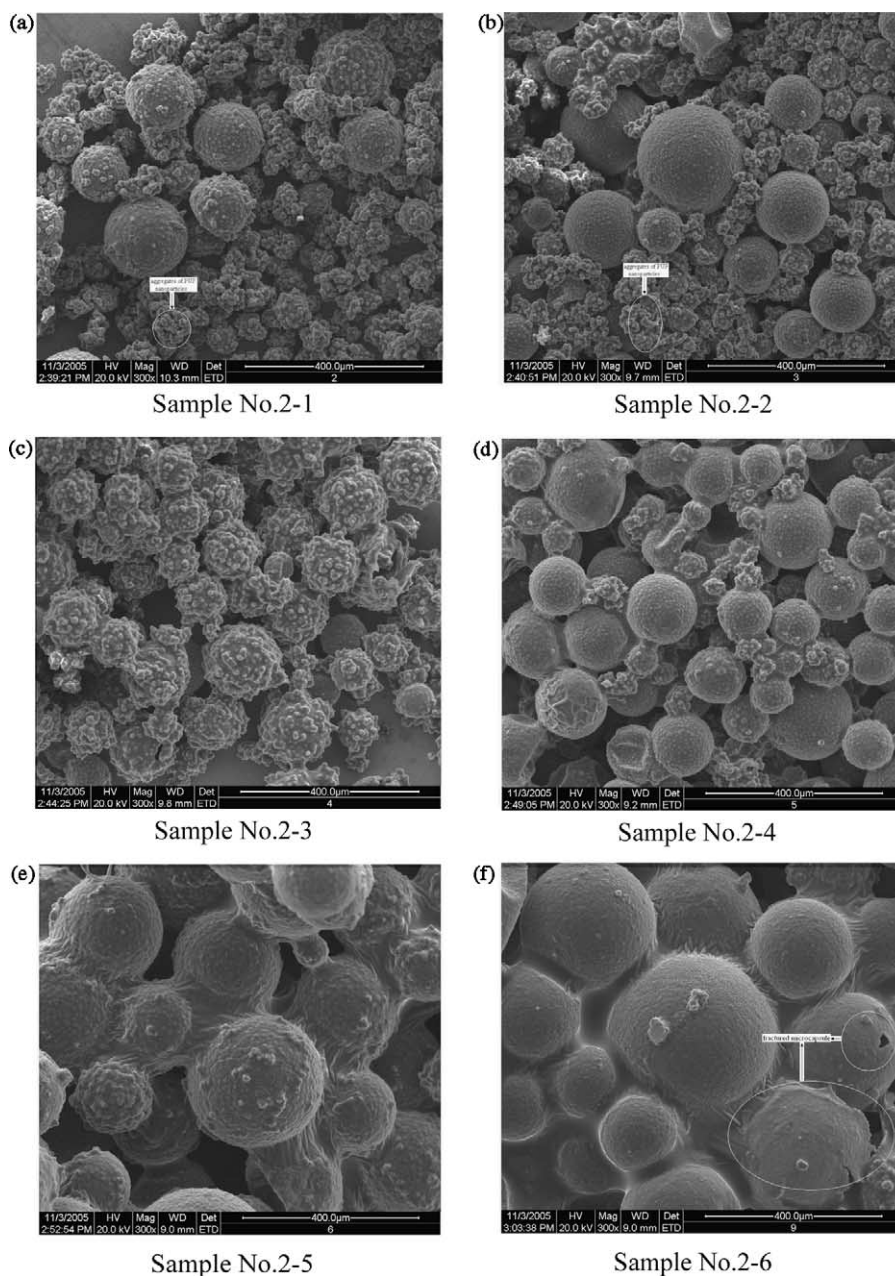


Fig. 13. SEM micrographs of microcapsules with different ratios of shell–core material (samples no. 2–1 to 2–6).

microcapsule, forming rougher and more porous outer layer of the PUF shell. Because the completion of condensation reaction for the higher U–F weight ratio resins needs longer time compared with the lower U–F weight ratio resins, the completion of microencapsulating core with the higher U–F weight ratio resins also needs more time. As a result, the core material cannot be microencapsulated completely by selecting higher U–F weight ratio resins when the other processing parameters are kept constant, and the yield of microcapsules decreases significantly for microcapsule sample no. 1–1 as shown in Table 1. The core contents of samples no. 1–1, 1–2 and 1–3 calculated according to Eqs. (2) and (3) are 72.3, 77.6 and 76.5%, respectively. The pre-polymers prepared by selecting different U–F weight ratios have no regular influence

on the core content, which depends on many processing parameters such as the weight ratio of core–shell material, the processing time and so on.

### 3.7. Effects of initial ratio of core–shell material

The effects of different initial weight ratios of core–shell material (samples no. 2–1 to 2–6) on the size and morphology of microcapsules were investigated. The initial weight ratio of core–shell material is varied from 0.50 to 2.00. Fig. 12 shows the relationship of initial weight ratios of core–shell material to microcapsule size. The diameters of microcapsules increase with the enhancement of weight ratio of core–shell material. The main reason is that the size of core droplet in emulsion is



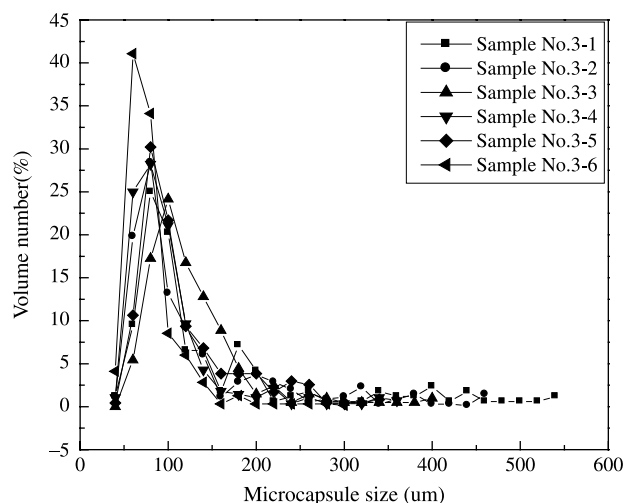


Fig. 14. Size distributions of microcapsules prepared at different agitation rates (samples no. 3–1 to 3–6).

larger when the weight ratio of core–shell is higher and the other processing parameters are kept constant. Although the wall shell thickness may decrease owing to the increase of core material, it slightly affects the diameter of microcapsule when the core material changes largely. Increasing the core material can form larger size core droplet, and accordingly, the microcapsule size becomes larger. But excess core materials cause poor dispersion, promoting aggregation of core droplets, resulting in lower yield of microcapsule sample no. 2–6 as shown in Table 1. Moreover, the microcapsules prepared by selecting higher weight ratio of core–shell material are easily fractured due to the thinner wall shell.

Fig. 13 shows the SEM micrographs of microcapsules, indicating that the surface of microcapsule becomes smooth with the increase of core material. It can be explained by the fact that increasing core material can reduce the deposition amount of PUF on each microcapsule and the aggregated fragments of PUF nanoparticles, and accordingly, the core

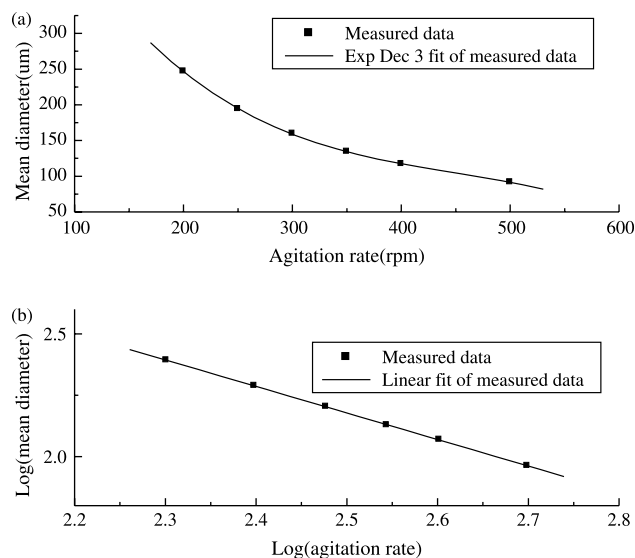


Fig. 15. Mean diameter vs. agitation rate (samples no. 3–1 to 3–6).

content of microcapsule increases as shown in Table 1. The yields of microcapsules prepared by selecting excessive wall shell material (samples no. 2–1, 2–2) or core material (sample no. 2–6), which are shown in Table 1, are lower than that of other microcapsule samples. The reason is that the excessive agglomeration of PUF occurs when selecting lower core–shell weight ratio, and microcapsules are easily fractured due to the thinner wall shell when selecting higher core–shell weight ratio as shown in Fig. 13(a), (b) and (f). Here, the optimal weight ratio of core–shell material is 1.00–1.25.

### 3.8. Mechanical effects on microcapsules

Fig. 14 shows the size distributions of microcapsules prepared by selecting different agitation rate from 200 to 500 rpm (samples no. 3–1 to 3–6). As the agitation rate increases, the microcapsule size distribution becomes narrow, the microcapsule size decreases and the smaller microcapsules become dominant, which are in accordance with the results reported by the Ref. [37]. The reason is that the oily droplets come under larger shear stress and their sizes are smaller when the agitation rate is higher, and accordingly, the prepared microcapsule diameters become smaller.

Fig. 15 shows various mean diameters of microcapsules prepared at different agitation rate in the range of 200–500 rpm (samples no. 3–1 to 3–6). As the agitation rate increases, a finer emulsion is obtained and the mean microcapsule diameter decreases. Adjusting agitation rates between 200–500 rpm can produce microcapsules with mean diameter in the range of 92–247  $\mu\text{m}$ . The relationship between mean diameter and agitation rate is third exponential decay as shown in Fig. 15(a) and linear in log–log scale as shown in Fig. 15(b), according well with the results reported by the Ref. [11].

Fig. 16 shows surface morphologies of microcapsules prepared at different agitation rate, which indicates the surface of microcapsule gradually becomes smooth with the increase of agitation rate. This phenomenon accords well with the results reported by the Ref. [11]. There are two main reasons for it. The first one is the higher agitation rate can lead to a relatively slow deposition rate and compact deposition of PUF nanoparticles on the surface of microcapsule. The second one is the higher agitation rate may reduce the conglomeration of PUF nanoparticles.

The core contents of microcapsule samples no. 3–1 and 3–2 prepared at lower agitation rate are higher than that of microcapsule samples no. 3–3, 3–4, 3–5 and 3–6 prepared at higher agitation rate (shown in Table 1). The reason is that the larger microcapsules are dominant when the agitation rate is lower, and the weight fraction of core material in larger microcapsule is relatively higher. Whereas the smaller microcapsules become dominant when the agitation rate is higher, and accordingly, the core weight fraction in smaller microcapsule is relatively smaller.

The yield of microcapsules enhances as the agitation rate increases from 200 to 350 rpm, and then decreases slightly as the agitation rate increases from 400 to 500 rpm (shown in Table 1). The reason is that increasing the agitation rate from

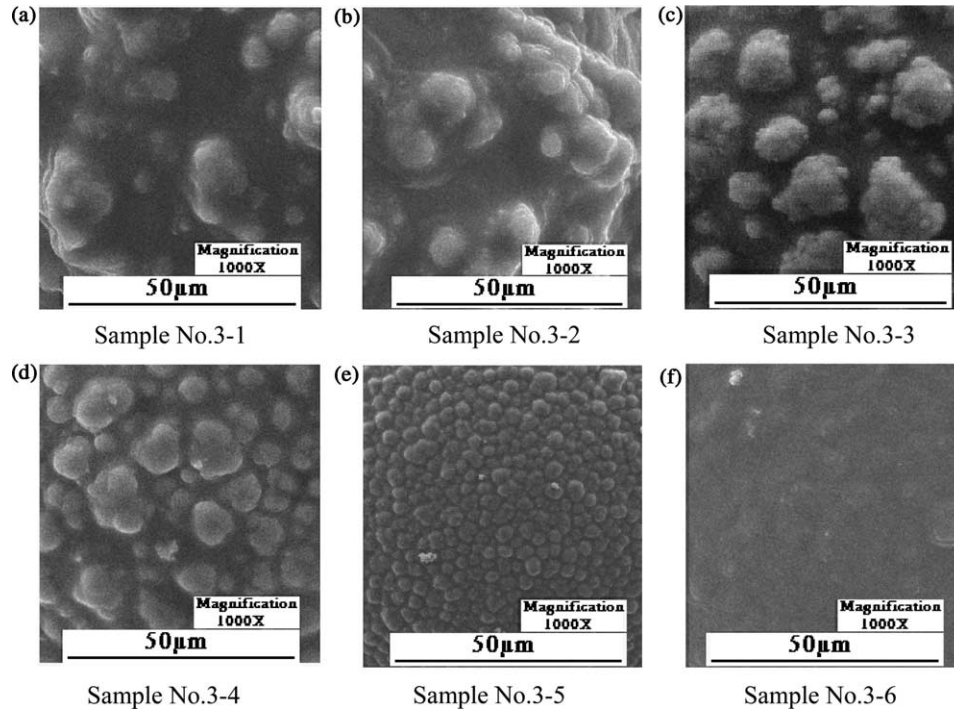


Fig. 16. Surface morphologies of microcapsules (samples no. 3–1 to 3–6).

200 to 350 rpm can reduce the aggregation of core droplets, decrease the amount of deformed microcapsules. When the agitation rate is higher ( $>350$  rpm), a few of larger microcapsules are affected significantly by the shear stress and they are fractured easily, which tend to decrease the yields of microcapsules.

### 3.9. Stability of microcapsules

Fig. 17 shows the relationships of stability of microcapsules between storage time and temperature (sample no. 1–2). The weight loss of microcapsules exposed to room temperature for 50 days is about 0.23 wt%, and as the exposed time increases further, the weight loss of microcapsules obviously becomes larger, indicating that the PUF microcapsules exposed to room temperature can maintain well in 50 days. The weight loss of microcapsules heat-treated increases with the enhancement of heating temperature and time, indicating that the microcapsules cannot be exposed to heat surrounding timelessly, which cause the larger weight loss of microcapsules. The main reason of weight loss of microcapsules at different temperatures is the elimination of free-formaldehyde and the diffusion of core material throughout the wall shell [38].

The thermal stability of microcapsules plays an important role in their applications in self-healing composites. Fig. 18 shows the DSC diagram of microcapsule sample no. 1–2. Two endothermic peaks and two exothermic peaks appear in the DSC curve of microcapsules. For the two endothermic peaks, the first endothermic one below  $100$  °C is due to the evaporation of water and free formaldehyde. The second one at temperatures between  $238$  and  $250$  °C is due to the

decomposition of shell materials [39]. As respect to the two exothermic peaks, the first one at about  $252$  °C is due to the polymerization reaction of core material, which is triggered by urea-derivatives and the gaseous products such as ammonia, monomethylamine and trimethylamine yielded by PUF shell material and the self-condensation of core material [39,40,41]. The second one above  $300$  °C, which cannot be observed completely on DSC curve, may be due to the continuous polymerization reaction of core material. Fig. 19 shows TGA

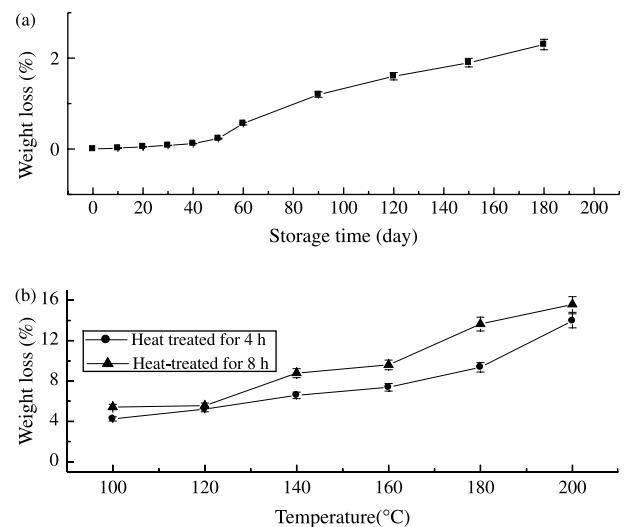


Fig. 17. Relationships of stability of microcapsules between storage time and temperature. (a) Weight loss of microcapsules at periodic intervals at room temperature. (b) Weight loss of microcapsules heat-treated for 4 and 8 h at different temperatures.

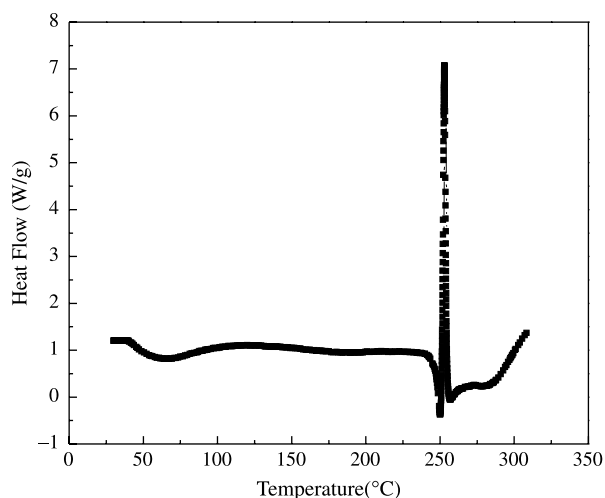


Fig. 18. DSC diagram of PUF microcapsules.

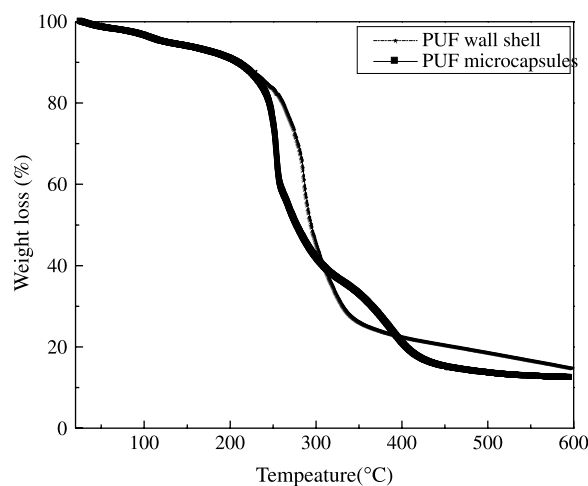


Fig. 19. TGA diagrams of PUF wall shell material and PUF microcapsules.

diagrams of microcapsule sample no. 1–2 and PUF wall shell material. TGA curve of PUF wall shell indicates that the weight loss near 100 °C is mainly due to the removal of entrapped residual water and the elimination of free formaldehyde [38], and the weight loss at temperatures between 238 and 300 °C is mainly due to the decomposition of the PUF wall shell. Due to the formation and the higher thermal stability of cross-linked polymer yielded by the core material, the weight loss of microcapsules in the range of 300–400 °C tends to decrease and the slope of TGA curve becomes small, compared with TGA curve of PUF wall shell material. The residuals undergo extensive fragmentation above 400 °C. Obviously, the thermal degradation of PUF microcapsule containing DGEBA and BGE is more complicated than that of PUF wall shell material. Weight loss temperature (5 wt% weight loss percentage) of the microcapsule samples is about 122 °C, and basically, the microcapsules are chemically stable below 238 °C, indicating that the prepared microcapsules have a good thermal stability.

#### 4. Conclusions

Microcapsules filled with DGEBA and BGE by in situ polymerization of urea–formaldehyde in an oil-in-water emulsion were prepared to develop the self-healing composites. In this study, the microcapsules were manufactured by selecting ultimately acid pH of 3–4 at 60–65 °C and different processing parameters. During the microencapsulation process, the epoxy resins are hardly affected by the surrounding media and the use of microcapsules is potential. The rough outer surface of microcapsule is composed of PUF nanoparticles. The size and the surface morphology of microcapsule can be adjusted by selecting different U–F pre-polymer, weight ratio of U–F and agitation rate. The relationship between mean diameter and agitation rate is third exponential decay and linear in log–log scale. The PUF microcapsules filled with DGEBA and BGE may have good storage at room temperature and basically exhibit a good chemical stability below 238 °C, which can withstand the moderate or high temperature processing of polymeric composites such as thermoset materials based on the epoxy resins. In general, this research provides novel microcapsules for the self-healing composites and the effects of the microcapsules on the polymeric composites will be further examined in our future study.

#### Acknowledgements

The work was supported by the special research foundation of doctoral subject from the education department of high school (20050699034) and the graduate starting seed fund of Northwestern Polytechnical University (Z200584).

#### References

- [1] Biju SS, Saisivam S, Maria NS, Rajan G, Mishra PR. *Eur J Pharm Biopharm* 2004;58(1):61.
- [2] Yutaka U, Kenichi H, Kageyosi S, Kazunori A, Yoshikazu T, Mutsuo S. *Surgery* 2001;130(3):513.
- [3] Yúfera M, Fernández-Díaz C, Pascual E. *Aquaculture* 2005;248(1–4):253.
- [4] Giraud S, Bourbigot S, Rochery M, Vroman I, Tighzert L, Delobel R. *Polym Degrad Stab* 2002;77(2):285.
- [5] Krishnan S, Bhosale R, Singhal RS. *Carbohydr Polym* 2005;61(1–4):95.
- [6] Kim CA, Joung MJ, Ahn SD, Kim GH, Kang SY, You IK, et al. *Synth Met* 2005;151(3):181.
- [7] Guo HL, Zhao XP. *Opt Mater* 2004;26(3):297.
- [8] Ji HB, Kuang JG, Qian Y. *Catal Today* 2005;105(3–4):605.
- [9] Sawada K, Urakawa H. *Dyes Pigments* 2005;65(1):45.
- [10] Yamamoto T, Dobashi T, Kimura M, Chang CP. *Colloids Surf, B* 2002;25(4):305.
- [11] Borwn EN, Kesslers MR, Sottost NR, White SR. *J Microencapsulation* 2003;20(6):719.
- [12] White SR, Sottos NR, Geubelle PH, Moore JS, Kessler MR, Sriram SR, et al. *Nature* 2001;409:794.
- [13] Kessler MR, Sottos NR, White SR. *Composites Part A* 2003;34(8):743.
- [14] Jung D, Hegeman A, Sottos NR, Geubelle PH, Whites SR. *Compos Funct Grad Mater* 1997;80:265.
- [15] Lee H, Neville K. *Handbook of epoxy resin*. New York: McGraw Hill; 1967.
- [16] Riccard CC, Adabbo HE, Williams RJ. *J Appl Polym Sci* 1984;29:2481.

- [17] Ellis B. Chemistry and technology of epoxy resins. London: Blackie Academic and Professional; 1993.
- [18] Orr CA, Cernohous JJ, Guegan P, Hirao A, Jeon HK, Macosko CW. Polymer 2001;42:8171.
- [19] Liu WC, Varley Russell J, Simon George P. Polymer 2006;47:2091.
- [20] Francis B, Thomas S, Jose J, Ramaswamy R, Lakshmana Rao V. Polymer 2005;46:12372.
- [21] Wang DZ, editor. Production and applications of epoxy resins. 2nd ed. China: Chemical Industry Press; 2002.
- [22] Dietrich K, Herma H, Nastke R, Bonatz E, Teige W. Acta Polym 1989;40:243.
- [23] Tan HS, Ng TH, Mahabadi HK. J Microencapsulation 1991;8:525.
- [24] Yan N, Ni P, Zhang M. J Microencapsulation 1993;10:375.
- [25] Taylor GI. Proc R Soc London, Ser A 1932;138:41.
- [26] Dobbetti L, Pantaleo V. J Microencapsulation 2002;19:139.
- [27] Pearce PJ, Morris CEM, Ennis BC. Polymer 1996;37(7):1137.
- [28] Zhang BL, Zhang HQ, You YC, Du ZG. J Appl Polym Sci 1998;69:339.
- [29] Lu SR, Zhang HL, Zhao CX, Wang XY. Polymer 2005;46:10484.
- [30] Ennis BC, Davidson RG, Paerce PJ, Morris CEM. J Adhesion 1992;37:131.
- [31] Leadley SR, Watts JF, Blomfield CJ, Lowe C. Surf Interface Anal 1998;26:444.
- [32] Watts JF, Abel ML, Perruchot C, Chris L, Maxted JT, White RG. J Electron Spectrosc Relat Phenom 2001;121:233.
- [33] González M, Kadlee P, Stepanek P, Streachota A, Matejka L. Polymer 2004;45:5533.
- [34] Cabanelas JC, Serrano B, Gonzalez MG, Baselga J. Polymer 2005;46:6633.
- [35] Pshenitsyna VP, Molotkova NN, Frenkel' MD, Tikhomirova YeYe, Gurman IM, Aksel'rodB Ya, et al. Polym Sci USSR 1979;21(9):2145.
- [36] He GB, Yan N. Polymer 2004;45:6813.
- [37] Kawashima Y, Niwa T, Handa T, Takeuchi H, Iwamoto T, Itoh K. J Pharm Sci 1989;78(1):68.
- [38] Zhang XX, Tao XM, Yick KL, Wang XC. Collid Polym Sci 2002;282:330.
- [39] Camino G, Operti L, Trossarelli L. Polym Degrad Stab 1983;5(3):161.
- [40] Galià M, Mantecoon A, Càdiz V, Serra A. Makromol Chem 1990;191:1111.
- [41] Wang MS, Pinnavaia TJ. Chem Master 1994;6:468.